

Nonlinear r -modes in neutron stars: A hydrodynamical limitation on r -mode amplitudes

Lap-Ming Lin^{1,2} and Wai-Mo Suen^{2,3}

¹ *Laboratoire de l'Univers et de ses Théories, Observatoire de Paris, F-92195 Meudon Cedex, France*

² *McDonnell Center for the Space Sciences, Department of Physics, Washington University, St. Louis, Missouri 63130, USA*

³ *Department of Physics, The Chinese University of Hong Kong, Hong Kong, China*

30 October 2018

ABSTRACT

Previously we found that large amplitude r -modes could decay catastrophically due to nonlinear hydrodynamic effects. In this paper we found the particular coupling mechanism responsible for this catastrophic decay, and identified the fluid modes involved. We find that for a neutron star described by a polytropic equation of state with polytropic index $\Gamma = 2$, the coupling strength of the particular three-mode interaction causing the decay is strong enough that the usual picture of the r -mode instability with a flow pattern dominated by that of an r -mode can only be valid for the dimensionless r -mode amplitude less than $O(10^{-2})$.

Key words: hydrodynamics - instabilities - gravitational waves - stars: neutron - stars: rotation

1 INTRODUCTION

The r -mode instability (Andersson 1998; Friedman & Morsink 1998) in rotating neutron stars has attracted much attention due to its possible role in limiting the spin rates of neutron stars and the possibility of producing gravitational waves detectable by LIGO II. However, the significance of this instability depends strongly on the maximum amplitude to which the r -mode can grow. A number of damping mechanisms of the r -mode have been examined, but no definite conclusion of the maximum amplitude can be made (see Andersson & Kokkotas (2001); Friedman & Lockitch (2001) for reviews; see also Andersson (2003) and references therein for a discussion of recent developments).

In Ref. (Gressman et al. 2002), we reported that large amplitude r -modes are subjected to a *hydrodynamic* instability that worked against the gravitational-radiation driven instability. Our numerical simulations showed that, for an r -mode with a large enough amplitude (e.g., with a dimensionless amplitude parameter α of order unity), the hydrodynamic instability operated in a timescale much shorter than that of the gravitational-radiation driven instability. This hydrodynamic instability when fully developed will cause the r -mode to decay catastrophically. As a result, the neutron star changes rapidly from the uniformly rotating r -mode pattern to a complicated differential rotating configuration. However, we have not been able to identify the hydrodynamic mechanism responsible for this catastrophic decay.

In this paper we establish that this catastrophic decay is

due mainly to a particular three-mode coupling between the r -mode and a pair of fluid modes. We identify the daughter modes and show that their frequencies satisfy a resonance condition: the sum of their frequencies is equal to the r -mode frequency. The importance of three-mode coupling in the r -mode evolution was first pointed out by Arras et al. (2003). By comparing the fully nonlinear simulation with the second-order perturbation equations, we determined the responsible mode coupling strength κ . The value of κ implies that this particular three-mode coupling alone gives a rather stringent limit to the usual picture of a neutron star with a fluid flow pattern dominated by the r -mode: Such a picture can only be valid with the dimensionless r -mode amplitude α smaller than or of the order 10^{-2} . Beyond that, the r -mode must be considered to be strongly coupled to other fluid modes. Instead of the gravitational radiation reaction, it is the fluid coupling that dominates the dynamics of the r -mode when its amplitude grows to 10^{-2} . Its evolution is strongly affected by the fluid coupling in a timescale much shorter than its growth time due to the gravitational-radiation driven instability. In particular, at that point the steady rise in amplitude of the r -mode due to gravitational radiation reaction will turn into a catastrophic decay. This is the main conclusion of the paper.

What happens after the catastrophic decay? As the post-decay fluid flow involves couplings between a large number of short wavelength modes beyond the resolution of our simulation, we cannot rule out the possibility that the r -mode can regain energy from these fluid modes and be revived within a hydrodynamic timescale (for a detailed study

arXiv:gr-qc/0409037v2 30 May 2006

of such “bouncing” phenomena see Brink et al. (2005)) before the star returns to uniform rotation. However, we do not see any hint of such bouncing in our simulations with an r -mode amplitude of order unity. This observation together with the consideration that a large number of fluid modes are involved in the catastrophic decay, lead us to conjecture that there is no such “bouncing” of the r -mode amplitude after the catastrophic decay.

We further note that there could be fluid modes with wavelengths shorter than what our numerical simulation can resolve but with couplings to the r -mode strong enough that place a stronger limit on the r -mode amplitude, as argued by Arras et al. (2003) and Brink et al. (2005). However, the bound we establish in this paper already has significant implications on the astrophysical importance of the r -mode instability.

The study in this paper makes no particular assumption on the neutron star model. The star is described simply as a self-gravitating, perfect-fluid body with a generic equation of state (a polytropic EOS); no dissipative mechanism is assumed. We have seen the same hydrodynamic phenomenon in simulations with stellar models of different central densities and polytropic indices. This suggests that the hydrodynamic mechanism being studied is quite generic.

2 NUMERICAL RESULTS

2.1 Nonlinear mode coupling

We solve the Newtonian hydrodynamics equations for a non-viscous, self-gravitating fluid body in the presence of a current quadrupole post-Newtonian radiation reaction (Gressman et al. 2002). We refer the reader to Gressman et al. (2002) for the neutron star model used in this study; and a detailed discussion on how we set up a large amplitude r -mode as an initial state for simulation. To set the stage for the study in this paper, we show in Fig. 1 the evolution of the r -mode amplitude α vs. time for the case where the initial nonlinear r -mode configuration has amplitude $\alpha = 1.6$. We compare the results for three different grid resolutions 129^3 , 161^3 , and 193^3 . The inset in Fig. 1 shows the details of the evolution in the time interval (15 ms-25 ms). Fig. 1 shows that α starts off slowly decaying until $t \approx 40$ ms (in the 193^3 simulation) at which point it decays catastrophically.

To investigate what hydrodynamic effect is responsible for the catastrophic decay of α , we divide the slowly decaying phase into a few time intervals, and study the Fourier spectra of the velocity fields. In Fig. 2 (a), we plot the Fourier transform of the axial velocity v^z along the x axis at $x = 2.56$ km inside the star for the 129^3 result plotted in Fig. 1. The dashed line is the Fourier spectrum of the earlier part of the evolution (13 ms-35 ms), while the solid line represents that of the later part (35 ms-50 ms). We see that the dashed line has only one large peak at the r -mode frequency ($r_0 = 0.93$ kHz). This is compared to the spectrum at the later time slot showing many peaks at different frequencies. In particular, we see a significant peak at 0.53 kHz.

Fig. 2 (b) shows the corresponding Fourier transforms of the rotational velocity v^y along the x axis at the same point as in Fig. 2 (a). In contrast to Fig. 2 (a), there is no peak at

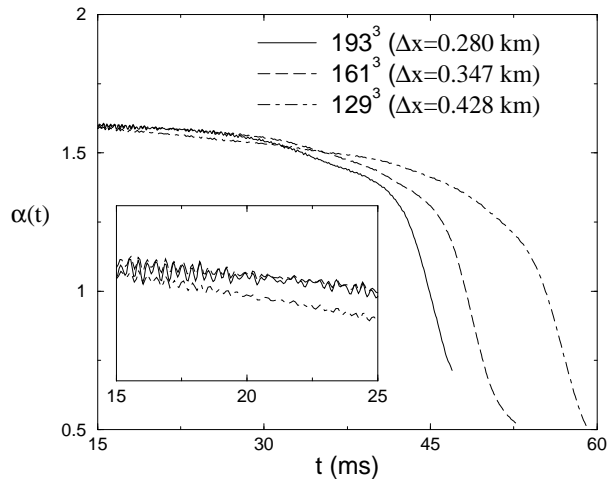


Figure 1. Evolution of α with initial value 1.6 with three different resolutions. The inset shows the details of the evolution between 15 ms-25 ms. In the 193^3 simulation, the neutron star is represented by a total number of $\approx 4.4 \times 10^5$ grid points.

the r -mode frequency r_0 in the initial time interval (dashed line). This shows that during the initial evolution the large amplitude r -mode maintains its character as given in the linear theory: no v^y component on the equatorial plane. In the later time interval (solid line), we see various peaks, and in particular a significant one at 0.40 kHz. It is also interesting to note the appearance of the peak at the r -mode frequency r_0 in the later time evolution. This is consistent with the formation of the large-scale vortex of the r -mode flow pattern during the late time evolution as reported in Gressman et al. (2002). The r -mode flow pattern changes rapidly to a vortical motion on the equatorial plane at the time when α collapses rapidly.

Figs. 2 (a) and (b) demonstrate that the r -mode can leak energy to other fluid modes through nonlinear hydrodynamic couplings, and in particular leaks energy to the fluid modes at frequencies 0.53 (henceforth the “A” mode) and 0.40 kHz (the “B” mode). Note that the sum of the frequencies of the A and B modes exactly equals to the r -mode frequency ($r_0 = 0.93$ kHz). This relation suggests that the r -mode leaks energy to this pair of modes via a three-mode coupling mechanism satisfying the resonance condition (Craik 1985)

$$f_A + f_B = f_R, \quad (1)$$

where the f ’s are the mode frequencies.

How do the coupled fluid modes grow? Instead of just two time slots, we can further divide the slowly decaying phase of α into several subintervals and perform Fourier transform on each of them, and monitor the Fourier amplitudes of different time intervals. In Fig. 3, we plot the Fourier amplitude of the A mode vs time for the case $\alpha = 1.2$ with resolution 193^3 . In the figure, the circles connected by a solid line are numerical data. The first data point corresponds to the Fourier amplitude obtained in the time interval 10 ms-25 ms. The time value of the data point (17.5 ms) is taken to be the middle of this interval. The second data point corresponds to 15 ms-30 ms, etc. The dashed line is fitted to the exponential function $f = A_0 \exp((t - 17.5)/9.35)$, where

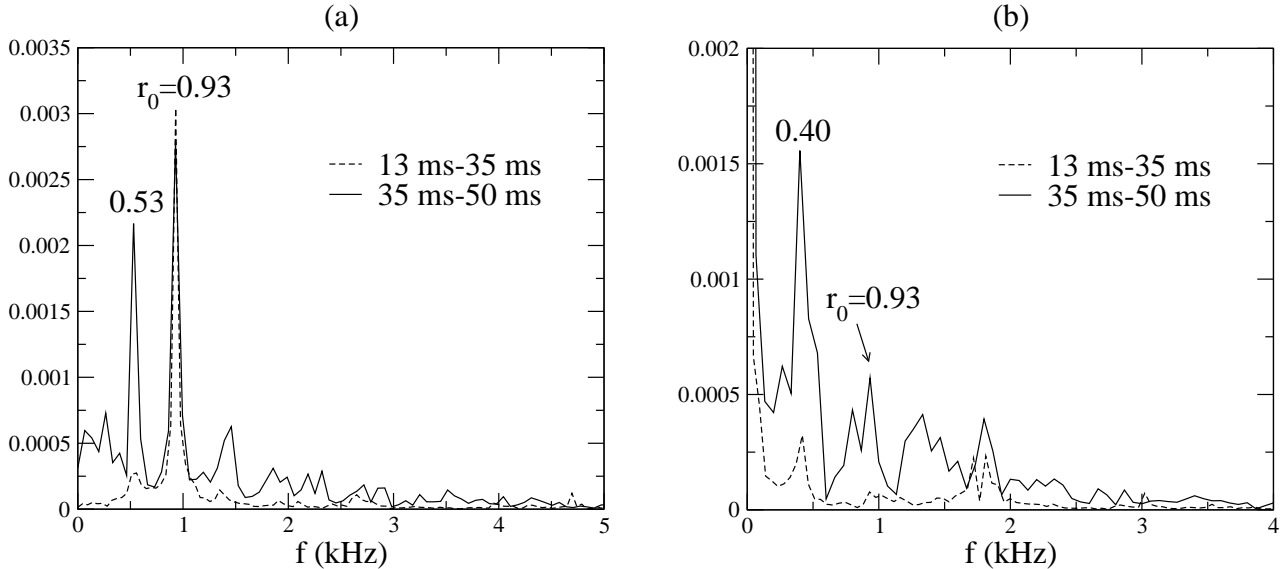


Figure 2. (a): Fourier spectra of v^z along the x axis (at $x = 2.56$ km) in the evolution of Fig. 1 at two time slots in the 129^3 simulation. (b): Fourier spectra of v^y for the same case.

t is in millisecond and A_0 is the Fourier amplitude obtained in the interval 10 ms-25 ms. Fig. 3 shows that the A mode grows exponentially with a time constant ≈ 9.35 ms during the slowly decaying phase of α . The B mode grows exponentially with a time constant about 7 percents larger as determined numerically.

Our results thus show that the coupled fluid modes are unstable and grow exponentially due to their couplings to the r -mode. An important point that we observed in all cases studied is that when the amplitudes of these two coupled daughter modes grow to a point comparable to that of the r -mode, the catastrophic decay of the r -mode sets in.

2.2 Determination of the Decay Rate of α

In the slowly decaying phase of α , there are two mechanisms that lead to the decay of α in our numerical simulation: (i) numerical damping arising from finite differencing error, which depends on the resolution used in the simulation; and (ii) physical damping due to the nonlinear interactions of the r -mode to other fluid modes, which depends on α at that moment. Fig. 1 shows that numerical damping is negligible during the early part (15 ms-30 ms) of the evolution at high enough resolutions. The 161^3 and 193^3 results agree to high accuracy. We can thus regard the rate of change of the r -mode amplitude $d\alpha/dt$ in the 193^3 simulation as a reasonable approximation to its physical value (when $\Delta x \rightarrow 0$) due to the particular three-mode coupling seen in our simulation. A linear curve-fit yields

$$\frac{d\alpha}{dt} = -2.9 \times 10^{-3} \text{ (ms)}^{-1}. \quad (2)$$

2.3 Determination of the waveforms

To further characterize the daughter modes, we would like to determine their waveforms in addition to their mode frequencies. However, this turns out to be non-trivial.

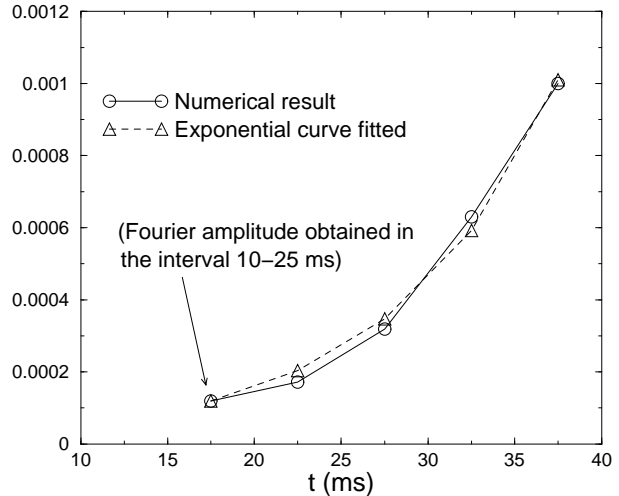


Figure 3. Exponential growth of the Fourier amplitude of the A mode for the case $\alpha = 1.2$ with resolution 193^3 .

In Fig. 4 (a), we show the v^z velocity profile for the 129^3 simulation shown in Fig. 1 along the x axis at $t = 28.88$ ms. We note that this is basically the velocity profile of the $m = 2$ r -mode. To extract the v^z waveform of the A mode, we need to subtract out the r -mode waveform. However, the r -mode waveform is known only in the linear approximation, while the r -mode being studied in this paper is not small and there can be non-linear correction to the r -mode waveform. To do the subtraction, we note that the non-linear correction should not change the symmetry of the r -mode, and in particular that its v^z is symmetric with respect to reflection about the origin on the x axis. We thus define the quantity $\Delta v^z := (v^z(x) - v^z(-x))/2$ on the x axis. In Fig. 4 (b), we plot Δv^z in the core region of the star at three different times for the 129^3 simulation shown in Fig. 1: $t = 28.88$ ms, $t = 29.82$, and $t = 30.76$ ms. The latter two time values differ from the first one respectively

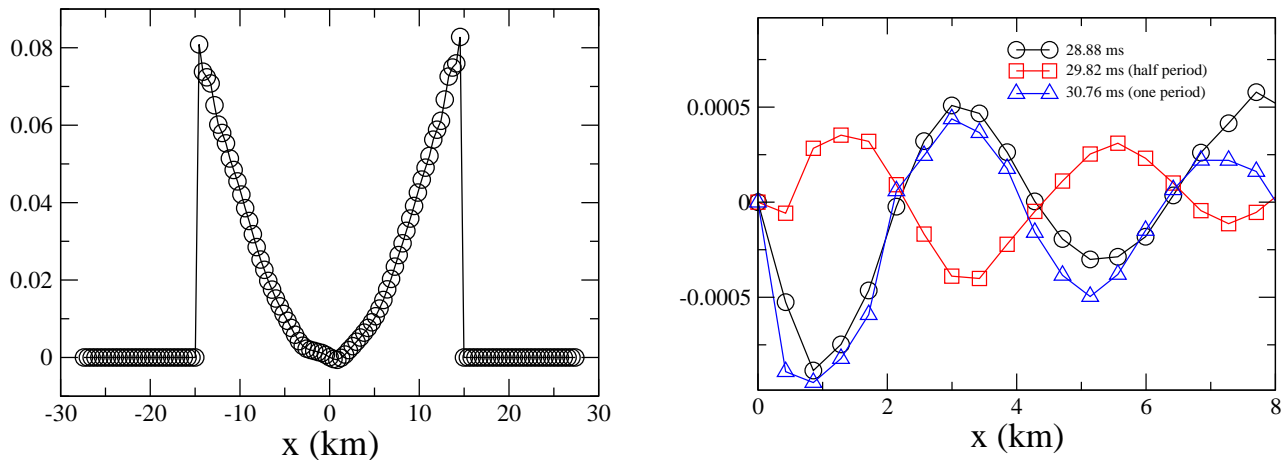


Figure 4. (a): The v^z velocity profile along the x axis at $t = 28.88$ ms for the 129^3 simulation shown in Fig. 1. (b): Waveforms of the A mode for the same case. Plotted are the profiles of Δv^z (see text) along the x axis at three different times. The latter two time values differ from the first one respectively by half and one oscillation period of the A mode.

by half and one oscillation period of the A mode (recall that $f_A = 0.53$ kHz). We see explicitly that the waveform oscillates with the frequency of the A mode. The two lines at $t = 28.88$ and 30.76 ms match pretty well, except in the region near the surface of the star where the r -mode velocity is large. This suggests that the extracted waveform is indeed the eigenfunction of the A mode. Note that the amplitude of the A mode is less than 1% of that of the r -mode in this early slowly-decaying phase. The extraction would not be possible without taking advantage of the symmetry.

Next we turn to the B mode, which is a mode with fluid flow in v^y . One might expect the waveform extraction to be easier, as the r -mode has no v^y component. To begin, we subtract the background rotation profile from the velocity component v^y by defining $\Delta v^y := v^y(x) - v_0^y(x)$ along the x axis, where v_0^y is the profile at the starting point of the slowly decaying phase of α . In Fig. 5, we plot Δv^y along the x axis at various times in the slowly decaying phase for the same 129^3 simulation as before. We see a small differential rotation pattern growing up to an amplitude a few percent of that of the r -mode. Four features of this fluid pattern are: 1. This differential rotation mode has a long period, much longer than that of the B mode. 2. The amplitude of this mode saturates at around 35 ms. 3. The energy of this mode is small comparing to the r -mode. 4. This mode is antisymmetric with respect to the origin along the x axis.

We uncovered a differential rotation pattern unrelated to the A and B modes. What is its significance? We make two observations: 1. One might suspect that this differential rotation pattern is part of the non-linear r -mode profile. It has been argued that differential rotation can be induced by second-order r -mode motion (e.g., Rezzolla et al. (2000); Sá (2004)) in perturbation analyses. However, the differential rotation pattern shown in Fig. 5 does not match those of (Rezzolla et al. 2000; Sá 2004). Further, we see that the differential rotation given in Fig. 5 is growing in amplitude during the slowly decaying phase of the r -mode. This suggests that it may not be part of the r -mode. 2. This differential rotation pattern is different from the one that developed during the catastrophic decay of the r -mode as we reported

previously (Gressman et al. 2002). Further investigations of this unknown mode (U mode) are needed.

To extract the B mode, we subtract the antisymmetric pattern of this “ U mode” and find a symmetric (with respect to reflection about the origin) v^y component with a period the same as that of the B mode. It is smaller than the U mode at earlier time, but overtakes the U mode in amplitude at around 40 ms. It keeps on growing exponentially to an amplitude comparable to that of the r -mode at the point of the catastrophic decay. In Fig. 6 we show the waveforms of the B mode (obtained by subtracting the U mode pattern from the profile of Δv^y) at around the time it becomes the dominant pattern. The two time slices 40.02 ms and 41.22 ms are separated by half of the oscillation period of the B mode, and indeed we see that the two lines are off by π in phase.

To summarize, we found an antisymmetric waveform in v^z for the A mode, and a symmetric waveform in v^y for the B mode. The wavelength of both modes are about 4 km in the central region of the star. Next we want to investigate if the symmetry properties of the waveforms of the modes are expected. We note that under a π -rotation (i.e., $\phi \rightarrow \phi + \pi$) on the equatorial plane, the Cartesian components of the velocity field of a toroidal fluid mode¹ transform according to $v^x \rightarrow (-1)^{m+1}v^x$, $v^y \rightarrow (-1)^{m+1}v^y$, and $v^z \rightarrow (-1)^m v^z$, where m is the azimuthal mode number (see Appendix A). This implies that the profiles of v^x and v^y along the x axis for an $m = -1$ mode are symmetric with respect to reflection about the origin; while the profile of v^z for an $m = -1$ mode is antisymmetric. We note that the A and B modes having

¹ Toroidal modes are characterized by fluid displacement vectors proportional to $\vec{r} \times \nabla Y_{lm}$, where Y_{lm} is the standard spherical harmonics. The r -mode is known to be a toroidal mode. We assume that the two daughter modes seen in our simulations are also toroidal modes (to leading order) because of their low frequencies compared to spheroidal modes (e.g., the f - and p -modes). The low frequency (spheroidal) g -modes do not exist in our isentropic simulations. But note that the inertial modes of isentropic stars in general have a “hybrid” nature (see Andersson & Kokkotas (2001) for discussion).

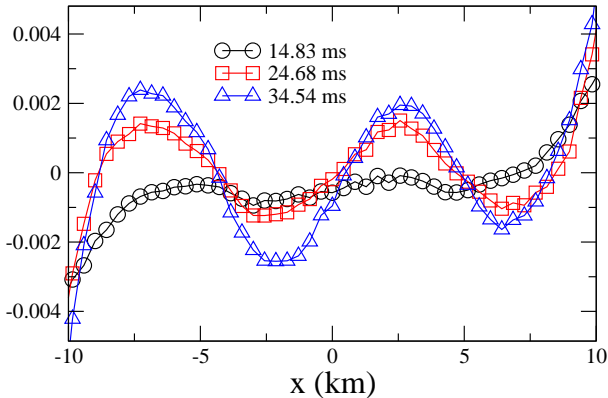


Figure 5. Differential rotation pattern Δv^y (see text) for the same simulation as Fig. 4.

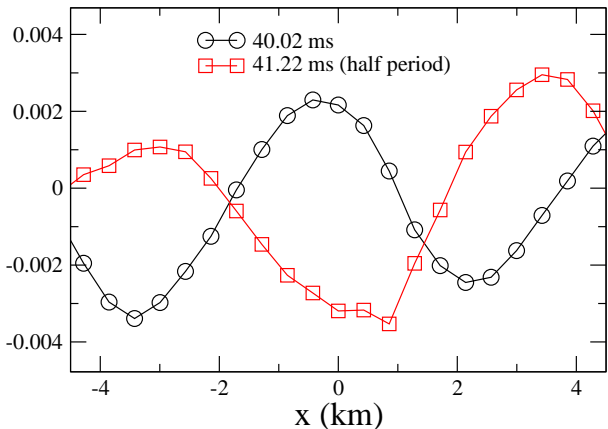


Figure 6. Waveforms of the B mode (see text) along the x axis at two different times (with a time interval half the oscillation period of the B mode) for the same simulation as Fig. 4.

$m = -1$ is consistent with the picture of three-mode coupling. The r -mode has $m = 2$ and the conservation of angular momentum requires that the azimuthal mode number m of the three coupled modes must satisfy $m_R + m_A + m_B = 0$ (Arras et al. 2003).

3 SECOND-ORDER PERTURBATION ANALYSIS

3.1 Three-mode coupling

The numerical results indicate that the dominant hydrodynamic contribution to the decay of the r -mode is due to its coupling to the A and B modes. To gain further insight into the hydrodynamic evolution during the early part of the numerical evolution, we compare the fully nonlinear simulation to a second-order perturbation analysis. In particular, we want to estimate the coupling strength of the three-mode coupling found, making use of the decay rate of α determined in Eq. (2). The second-order perturbation analysis enables us to extract information about the mode coupling independent of the specific value of α used in the numerical simulation. Through this we will then be able to determine the behavior of the r -mode at α values smaller than that

used in the simulations. Note that the following analysis only makes use of information obtained in the slowly decaying phase of α , where a second-order perturbation analysis is assumed to be valid. In particular, it does NOT depend on the existence of a catastrophic decay. The perturbation description is NOT expected to be valid when the evolution is getting near to the point of the catastrophic decay and beyond.

In a reference frame co-rotating with a rotating star, the second-order perturbation equations for a system of three modes in resonance can be written as (Schenk et al. 2001; Arras et al. 2003)

$$\frac{dq_R}{dt} + i\omega_R q_R = \frac{q_R}{\tau_R} + i\omega_R \kappa_{RAB}^* q_A^* q_B^*, \quad (3)$$

$$\frac{dq_A}{dt} + i\omega_A q_A = -\gamma_A q_A + i\omega_A \kappa_{RAB}^* q_R^* q_B^*, \quad (4)$$

$$\frac{dq_B}{dt} + i\omega_B q_B = -\gamma_B q_B + i\omega_B \kappa_{RAB}^* q_R^* q_A^*, \quad (5)$$

where the q 's represent the dimensionless complex amplitudes of the modes; the ω 's are the rotating frame angular frequencies of the modes; τ_R is the growth time of the r -mode due to radiation reaction; κ_{RAB} is the coupling strength; Z^* denotes the complex conjugate of Z ; γ_A and γ_B are the damping coefficients of the two coupled modes representing the outflow of energy from the three mode system.

The system of equations (3)-(5) gives rise to a resonant coupling for modes satisfying $\omega_A + \omega_B + \omega_R \approx 0$. Note that this is not inconsistent to the resonance relation (1) satisfied by the (inertial frame) frequencies of the coupled modes. The rotating frame angular frequency of a fluid mode ω is related to the inertial frame angular frequency ω_0 by $\omega = \omega_0 + m\Omega$, where Ω is the angular velocity of the star. For the star model ($\Omega = 4.87 \text{ (ms)}^{-1}$) and $m = 2$ r -mode with the inertial frame frequency $r_0 = 0.93 \text{ kHz}$ being studied, we have $\omega_R = 3.9 \text{ (ms)}^{-1}$. Note that we define ω_0 to be negative for the r -mode (see Gressman et al. (2002)). The rotating frame angular frequencies of the $m = -1$ daughter modes are respectively $\omega_A = -1.54 \text{ (ms)}^{-1} \approx -0.4\omega_R$ and $\omega_B = -2.36 \text{ (ms)}^{-1} \approx -0.6\omega_R$, suggesting that the three modes indeed satisfy the resonance condition $\delta\omega = \omega_A + \omega_B + \omega_R \approx 0$.

The meaning of the γ 's used here is somewhat different from that of Arras et al. (2003) and Brink et al. (2005). The neutron star EOS used in this paper is that of a perfect fluid with no viscosity. The γ 's describe the couplings of this particular three-mode system to the other fluid modes of the neutron star and is a function of the amplitude of these other modes. The description of Eqs. (3)-(5), is meaningful only when the γ 's are not changing in a time scale short compare to that of the dynamical time scales of the A , B and r modes, a point we will return to later in the paper.

A general expression for κ_{RAB} is given in Schenk et al. (2001). In writing the coupled equations above, we omit the coupling terms proportional to κ_{RAA} and κ_{RBB} , which are zero due to a z -parity selection rule (Schenk et al. 2001). This selection rule states that $\kappa_{ABC} = 0$ for an odd number of z -parity odd modes. Since the r -mode has odd z -parity, $\kappa_{RAA} = 0$ regardless of the z -parity of mode A . In order that $\kappa_{RAB} \neq 0$, modes A and B should have different z -parity. We see in our simulations that one of the coupled modes (A)

appears only in the Fourier spectrum of v^z , while the other one (B) appears only in the v^y spectrum.

Note that the definition of κ_{RAB} used by us is the same as Arras et al. (2003), but different from that used by Brink et al. (2005) (and also Schenk et al. (2001)). In our notation, κ_{RAB} is the ratio of the nonlinear interaction energy to the energy of the mode (both at unit amplitude). The conversion from our κ to the one used by Brink et al. (2005) is $\kappa \rightarrow E_{\text{unit}}\kappa$, where $E_{\text{unit}} = \frac{1}{2}MR^2\Omega^2$ is the mode energy at unit amplitude in the normalization used by them.

In order to relate q_R to the nonlinear r -mode amplitude defined in our numerical simulations we take $|q_R(t)| \simeq \alpha(t)$ (the critical amplitude α_{crit} given below applies as long as $|q_R|$ is proportional to α). Using Eq. (3) and its complex conjugate, it can be shown that α satisfies

$$\frac{d\alpha}{dt} = \frac{\alpha}{\tau_R} + \frac{\omega_R}{\alpha} \text{Im}(\kappa_{RAB}q_Aq_Bq_R), \quad (6)$$

where $\text{Im}(Z)$ denotes the imaginary part of Z . In the slowly decaying phase of α , $|q_A| \simeq |q_B| = q$ is less than $|q_R|$ (with the catastrophic decay sets in at $q \approx \alpha$). We obtain the following order-of-magnitude estimate for the coupling strength $|\kappa_{RAB}|$:

$$|\kappa_{RAB}| \sim \frac{1}{\omega_R q^2} \left| \frac{d\alpha}{dt} - \frac{\alpha}{\tau_R} \right| \sim 3 \times 10^{-4}, \quad (7)$$

where we have used $\alpha = 1.6$, $d\alpha/dt = -2.9 \times 10^{-3} \text{ (ms)}^{-1}$, $\omega_R = 3.9 \text{ (ms)}^{-1}$, $\tau_R = 40 \text{ s}$, and $q \approx \alpha$. Note that using a smaller value of q will only increase the value of $|\kappa_{RAB}|$. In this sense, the $|\kappa_{RAB}|$ given by Eq. (7) is a lower bound. A larger $|\kappa_{RAB}|$ gives a tighter bound to the r -mode amplitude at the point of catastrophic decay α_{crit} as shown below.

To check that the value of $|\kappa_{RAB}|$ does not depend sensitively on the initial value of α used in the simulation, we have repeated the above calculation with a different initial r -mode amplitude $\alpha = 1.2$. In that case, we obtain $d\alpha/dt = -1.7 \times 10^{-3} \text{ (ms)}^{-1}$ during the slowly decaying phase of α . The value of $|\kappa_{RAB}|$ changes only by a few percents (within numerical error) comparing to the case $\alpha = 1.6$.

To complete the description of the system using Eqs. (3)-(5), one would also like to determine from the numerical simulation the values of γ_A and γ_B . In our present setup, γ_A and γ_B determine the rate of energy leaking out of the three-mode system through coupling to other fluid modes. However, due to the constraint of computational resources we were not able to obtain the precise values of γ_A and γ_B since they correspond to a timescale orders of magnitude longer than 10 ms (the timescale of the growth of the daughter modes in our simulations), in the regime where the daughter modes A and B are small compared to the r -mode.

In our simulations, when the amplitudes of the two daughter modes become comparable to that of the r -mode, the perturbation equations (3)-(5) are no longer valid. The evolution becomes fully nonlinear, and the r -mode decays catastrophically at that point.

3.2 Amplitude of the R -mode at the catastrophic decay

Now we consider how an r -mode would evolve from a small initial amplitude to the decay point in a star described by

a perfect-fluid EOS, based on the fully nonlinear numerical simulation and information from the second-order perturbation analysis. We assume that during the early evolution the r -mode couples mainly only to the two resonant modes (A and B). In this phase, the system can be described by Eqs. (3)-(5). The A and B modes are negligible initially; the r -mode grows due to radiation reaction. When α becomes large enough, $|q_A|$ and $|q_B|$ grow rapidly. The point at which the two daughter modes catch up in amplitude with the r -mode can be estimated by setting $d\alpha/dt = 0$ in Eq. (6). In particular, the amplitude of the r -mode at that point is given by

$$\alpha_{\text{crit}} \sim \frac{1}{\omega_R \tau_R |\kappa_{RAB}|} \sim 0.02, \quad (8)$$

where we have taken $|q_A| \approx |q_B| \approx \alpha_{\text{crit}}$.

At this point, the usual picture of a neutron star with fluid flow dominated by an r -mode pattern is no longer valid. It is somewhat surprising that a single three-mode coupling of purely hydrodynamic nature could put a limit as strong as $\alpha \sim 0.02$. To the best of our knowledge this is the first explicit demonstration that an r -mode cannot be the dominant feature of a rapidly rotating neutron star with an amplitude beyond $\alpha \sim 0.02$.

The critical amplitude α_{crit} in Eq. (8) is defined to be the amplitude of the r -mode when nonlinear hydrodynamic couplings dominate the gravitational radiation reaction in driving the r -mode evolution; it is the time when the daughter modes catch up in amplitudes with the r -mode. It should be noted that this critical amplitude is different from the so-called parametric instability threshold (see, e.g., Eq. (2) of Brink et al. (2005)), which is defined to be the amplitude of the parent mode at the point when the two daughters become unstable due to nonlinear coupling and start to grow exponentially. The scalings of the two amplitudes are different. In particular, the parametric instability threshold does not depend on the growth time τ_R of the r -mode, while our critical amplitude α_{crit} is inversely proportional to τ_R .

3.3 Beyond the Critical Point

What happens after the point $\alpha = \alpha_{\text{crit}}$ is reached? Our numerical simulation shows that when the two daughter modes catch up in amplitude with the r -mode near α_{crit} , the following happen: 1. Many other fast growing fluid modes enter the picture. 2. The fluid flow can no longer be approximately described by the three-mode perturbation system Eqs. (3)-(5). 3. The r -mode decays catastrophically. 4. After the catastrophic decay, the neutron star has a complicated differential rotating flow pattern with short length scales, and 5. there is no sign of the r -mode re-gaining its energy from the many fluid modes it directly or indirectly coupled to.

One important implication of this is: The maximum amplitude α_{max} an r -mode can get to through the gravitational-radiation driven instability is given by $\alpha_{\text{max}} = \alpha_{\text{crit}}$. However, there is a caution: our simulation is carried out with α of order unity but not directly at $\alpha \sim 0.02$. There is a possibility that even though the fluid flow is no longer dominated by that of the r -mode after the two daughter modes catch up at $\alpha_{\text{crit}} \sim 0.02$, the three-mode perturbation system Eqs. (3)-(5) could remain a valid description of the neutron star. The perturbation system can fail to represent the flow of the

star for two reasons: (i) the mode amplitudes become large, so that higher order perturbation terms in the equations cannot be neglected, or (ii) the effects of modes other than the three modes studied become significant (this shows up also as the γ 's are changing on a short time scale); such a situation is strongly suggested by our simulation. Unfortunately simulations of timescales long enough to accurately capture the behavior of r -modes with a small α value require a computational resource beyond what is available to us, and we cannot investigate the catastrophic decay at small α value in full.

In case the second-order perturbation equations (3)-(5) are still valid at the point $\alpha = \alpha_{\text{crit}}$, what could happen subsequent to the catastrophic decay? In particular, can the amplitude of the r -mode evolve to a value substantially larger than α_{crit} ? The subsequent evolution described by Eqs. (3)-(5) depends strongly on the relative values of γ_A , γ_B , τ_R , and the frequency detuning $\delta\omega = \omega_A + \omega_B + \omega_R$. As discussed in Arras et al. (2003), a stable equilibrium solution of Eqs. (3)-(5) exists if both the damping and detuning are large: $\gamma_A + \gamma_B > \tau_R^{-1}$; $|\delta\omega| > (\gamma_A + \gamma_B)/2$. Otherwise, the system is unstable. (Note that in our study γ_A and γ_B represent the rate of energy leaking out of the three-mode system to other fluid modes of the neutron star, which is described by a perfect fluid EOS with no viscosity.)

In the case where a stable equilibrium solution exists, the system will settle into a steady state with the mode amplitudes being roughly the same. The maximum amplitude of the r -mode α_{max} would be given by α_{crit} . On the other hand, in the unstable case Eqs. (3)-(5) predict that after the amplitudes of the three coupled modes become comparable, the amplitudes of the three modes will fluctuate in a short timescale with rapid energy transfer between them, and the average amplitude of all three modes could grow until the second-order perturbation analysis becomes invalid. However, such oscillation of energy between the three modes is possible only if their phase relations are well preserved in the evolution, a condition we believe may not happen in realistic nonlinear hydrodynamic evolutions: at $\alpha \approx \alpha_{\text{crit}}$ a large number of other fluid modes enter into the picture and affect the fluid evolution significantly. The energy originally in the r -mode is transferred to many fluid modes. The involvement of a large number of modes suggests that the oscillation of energy back to the r -mode in a short dynamical timescale is unlikely. As an example, in a chain of N coupled nonlinear oscillators an equipartition of energy among the coupled modes is achieved if the energy of the initial large scale mode is larger than a certain threshold, which tends to zero sufficiently fast at increasing N (Casetti et al. 1997). This suggests that, after cascading its energy down to a sea of coupled modes, a generic initial large scale mode cannot regain its energy within dynamical timescale. We believe that this is also the case for nonlinear couplings of the r -mode to other fluid modes in rotating neutron stars. Hence, we *conjecture* that such oscillation of energy cannot occur beyond the catastrophic decay and the amplitude of the r -mode is bounded by α_{crit} .

Nevertheless, we do not rule out the possibility that the global r -mode could grow again in a secular timescale (~ 40 s) due to the driving of gravitational radiation reaction. We have extended some of our simulations for a timescale of 10 ms after the catastrophic decay. However, we do not see any

evidence of the regrowth of an unstable r -mode, even with an artificially enlarged radiation reaction force. One possibility is that the strong differential rotation developed during the catastrophic decay (see Gressman et al. (2002)) may act to stabilize the r -mode. If this is the case, it will take even a much longer time, until the differential rotation is damped out by viscosity (not modelled in our simulations), before the r -mode can grow again. To model such regrowth scenario, if it occurs at all, would be too expensive computationally for present-day technology. This is still an open issue and remains to be investigated in the future.

4 COMPARISON WITH OTHER WORK

There are two other numerical simulations of nonlinear r -modes, both finding that, large amplitude r -modes can exist for a long period of time. Stergioulas & Font (2001) performed relativistic simulations of the r -mode on a fixed spacetime background. They started with a large r -mode perturbation in a relativistic rotating star and evolved the system for about twenty rotation periods. They found no evidence of mode saturation unless the r -mode amplitude was much larger than unity. Lindblom et al. (2001) carried out numerical simulations of the growth of the r -modes driven by the current quadrupole radiation reaction in Newtonian hydrodynamics. To achieve a significant growth of the r -mode amplitude in a reasonably short computational time, they multiplied the radiation reaction force by a factor of 4500, decreasing the growth time of the r -mode from about 40 s to 10 ms. The r -mode amplitude α grew to ≈ 3.3 , before shock waves appeared on the surface of the star and the r -mode collapsed. They suggested that the nonlinear saturation amplitude of the r -modes might be set by dissipation of energy in the production of shock waves.

We note that, with the artificially large radiation reaction, the results in (Lindblom et al. 2001) assume that no hydrodynamic process takes energy away from the r -mode in a timescale between 10 ms and 40 s (the artificial growth time and the actual physical growth time, respectively). In our previous work (Gressman et al. 2002), we showed that r -modes of amplitudes unity or above were destroyed by a catastrophic decay within this time period. During the process the r -mode motion changed rapidly to a vortical motion and strong differential rotation developed. The mechanism leading to this catastrophic decay is studied in this paper.

Another approach to study the nonlinear couplings between the r -modes and other fluid modes is via perturbation theory. In this analytic approach, one assumes that the system is weakly interactive; and the r -mode couples to other fluid modes via the lowest order couplings so that higher order effects can be ignored. Based on a second-order perturbation theory developed by Schenk et al. (2001), Arras et al. (2003) proposed a turbulent cascade scenario in which the energy of the r -mode leaked to a large number of short wavelength inertial modes due to three-mode couplings. The coupled modes are in turn damped by viscosity. They argued that the rotating frame r -mode energy could be limited to $E_{r\text{-mode}} \approx 10^{-6} E_{\text{unit}}$ for a millisecond rotating star, where $E_{\text{unit}} = \frac{1}{2} MR^2 \Omega^2$. In their normalization, the r -mode amplitude (A_1 in their notation) was related to the mode energy by $E_{r\text{-mode}} = 2E_{\text{unit}} A_1^2$. Note that the normalization of the

r -mode amplitude α used by us (Gressman et al. 2002) is such that $A_1 \approx 0.09\alpha$ (see Sec. 8 of Arras et al. (2003)). Hence, in our notation, the maximum r -mode amplitude suggested by them is $\alpha \approx 8 \times 10^{-3}$.

In a recent second-order perturbative work, Brink et al. (2005) have studied the evolution of the unstable r -mode in a nonlinear network coupled with about 5000 inertial modes. They considered a uniform density, incompressible uniformly rotating star. With this simplified model, they calculated the eigenfunctions of the inertial modes and the three-mode coupling coefficient κ analytically. Their study suggested that, while the behavior of the r -mode was complicated and depended sensitively on the damping effects of the coupled modes, the r -mode amplitude would in general be limited to a small amplitude: $c_\alpha \approx 10^{-4}$ in their notation. Note that the normalization convention used by Brink et al. (2005) is such that the r -mode energy is given by $E_{r\text{-mode}} = E_{\text{unit}} c_\alpha^2$. This in turn gives the relation $c_\alpha = \sqrt{2}A_1 \approx 0.13\alpha$, and thus the r -mode is limited to $\alpha \approx 8 \times 10^{-4}$ in our notation.

In the perturbation studies of Brink et al. (2005), they found that beyond the critical point α_{crit} , energy might oscillate between the r -mode and the fluid modes it coupled to. After the catastrophic decay, the r -mode amplitude could re-grow to a value comparable to that just before the decay in a short timescale. In our numerical simulations with α of order unity, we do not see any such oscillations, instead the r -mode energy cascades into a large number of fluid modes beyond α_{crit} . We conjecture that such oscillations are not possible in fully nonlinear evolutions and realistic neutron stars. This conjecture in turns implies that the r -mode amplitude is limited to α_{crit} .

5 CONCLUSIONS AND DISCUSSIONS

In this paper, we identify a particular three-mode coupling between the r -mode and the pair of fluid modes responsible for the catastrophic decay of large-amplitude r -modes seen in our previous simulations (Gressman et al. 2002). The three modes satisfy a suitable resonance condition to high accuracy. This also demonstrates that hydrodynamic three-mode coupling can play an important role in the r -mode evolution as first pointed out by Arras et al. (2003). We have also extracted the eigenfunctions of the two daughter modes, and demonstrated that they are consistent with having azimuthal mode number $m = -1$.

While the fully nonlinear simulations are carried out with a large amplitude r -mode that is obtained by an artificially large gravitational radiation reaction, we succeed in drawing conclusions on the r -mode evolution at smaller amplitude through a comparison with a second-order perturbation analysis. In particular, we show that the three-mode equations (3)-(5) are valid in the simulation when the daughter modes are small, and determine the coupling strength $|\kappa_{RAB}|$ of this particular three-mode coupling to be (at least) $\sim O(10^{-4})$. This implies that the two daughter modes will catch up with the r -mode at a rather small amplitude ($\alpha = \alpha_{\text{crit}} \sim O(10^{-2})$), for an r -mode driven by gravitational radiation reaction. We conclude that at $\alpha \sim O(10^{-2})$ the usual picture of the fluid flow of the neutron star dominated by an r -mode would no longer be valid,

with many other modes significantly affecting the fluid flow leading to a catastrophic decay.

Our numerical simulations are limited to a spatial resolution of $\Delta x \sim 0.3$ km. Fluid modes with wavelengths smaller than $\lambda \sim 1$ km cannot be accurately represented. It is possible that the couplings of the r -mode to a large number of shorter wavelength modes can limit α_{crit} to an even smaller value (as suggested by Arras et al. (2003); Brink et al. (2005)). The amplitude for the catastrophic decay α_{crit} determined in this paper is as an upper bound.

The study in this paper is carried out with the neutron star described as a self-gravitating perfect fluid body with a polytropic equation of state. No particular dissipation mechanism is assumed. This suggests that the hydrodynamic behavior we see is of rather general nature.

Finally, we comment on future prospects of numerical investigations of the r -mode instability. An interesting question that one might ask is whether numerical simulations could be used to test the maximal amplitudes inferred in this paper by starting the r -mode evolution directly at $\alpha \sim \alpha_{\text{crit}}$ instead of $\alpha \sim O(1)$ as we have done in our simulations. As we have shown in Gressman et al. (2002), the time it takes for the r -mode to reach the point of catastrophic decay depends sensitively on the value of α . For $\alpha \sim \alpha_{\text{crit}}$, it would take a time much longer than what could be modelled accurately by our finite-differencing code in order to see a significant growth of the daughter modes and the catastrophic decay of the r -mode. Nevertheless, it might be possible to use hydrodynamics codes based on spectral methods (see, e.g., Villain & Bonazzola (2002)) to handle such long timescale problem, since spectral methods can achieve a much higher numerical accuracy in general for smooth fluid flow.

ACKNOWLEDGEMENTS

We thank the anonymous referees for useful comments which improve the paper. This research is supported in parts by NSF Grant Phy 99-79985 (KDI Astrophysics Simulation Collaboratory Project), NSF NRAC MCA93S025, the Research Grants Council of the HKSAR, China (Project No. 400803), and the NASA AMES Research Center NAS. L.M.L. acknowledges support from a Croucher Foundation fellowship.

REFERENCES

- Andersson N., 1998, ApJ, 502, 708
- Andersson N., 2003, Class. Quantum Grav., 20, R105
- Andersson N., Kokkotas K. D., 2001, Int. J. Mod. Phys. D, 10, 381
- Arras P., Flanagan E. E., Morsink S. M., Schenk A. K., Teukolsky S. A., Wasserman I., 2003, ApJ, 591, 1129
- Brink J., Teukolsky S. A., Wasserman I., 2005, Phys. Rev. D, 71, 064029
- Casetti L., Cerruti-Sola M., Pettini M., Cohen E. G. D., 1997, Phys. Rev. E, 55, 6566
- Craik A. D., 1985, Wave Interactions and Fluid Flows, Cambridge University Press
- Friedman J. L., Lockitch K. H., 2001, preprint (gr-qc/0102114)

- Friedman J. L., Morsink S. M., 1998, *ApJ*, 502, 714
 Gressman P., Lin L.-M., Suen W.-M., Stergioulas N., Friedman J. L., 2002, *Phys. Rev. D*, 66, 041303(R)
 Lindblom L., Tohline J. E., Vallisneri M., 2001, *Phys. Rev. Lett.*, 86, 1152
 Rezzolla L., Lamb F. K., Shapiro S. L., 2000, *ApJ*, 531, L139
 Sá P., 2004, *Phys. Rev. D*, 69, 084001
 Schenk A. K., Arras P., Flanagan E. E., Teukolsky S. A., Wasserman I., 2001, *Phys. Rev. D*, 65, 024001
 Stergioulas N., Font J. A., 2001, *Phys. Rev. Lett.*, 86, 1148
 Villain L., Bonazzola S., 2002, *Phys. Rev. D*, 66, 123001

APPENDIX A: TRANSFORMATION RULES OF TOROIDAL MODES

In this appendix, we derive the transformation rules for the Cartesian velocity components of toroidal modes on the equatorial plane. An arbitrary fluid displacement vector $\vec{\xi}$ can be decomposed in vector spherical harmonics as

$$\vec{\xi} = \sum_{lm} (A_{lm} Y_{lm} \hat{r} + B_{lm} \nabla Y_{lm} + C_{lm} \vec{r} \times \nabla Y_{lm}), \quad (\text{A1})$$

where $(\hat{r}, \hat{\theta}, \hat{\phi})$ is the coordinate vector basis associated with the spherical polar coordinates (r, θ, ϕ) ; $Y_{lm}(\theta, \phi)$ are the standard spherical harmonics; the quantities $A_{lm}(r)$, $B_{lm}(r)$, and $C_{lm}(r)$ are functions of r only. Fluid modes for which $C_{lm} = 0$ (for all l and m) are called spheroidal modes, while those for which $A_{lm} = B_{lm} = 0$ are called toroidal modes. Here we only consider the latter class of modes.

The spherical harmonics can be written as $Y_{lm} = b_{lm} e^{im\phi} P_l^m(\cos\theta)$, where b_{lm} is a constant depending on l and m , and P_l^m are the associated Legendre polynomials. For a fixed (l, m) component, we have the following angular dependence for torodial modes

$$\vec{\xi}_{lm} \sim e^{im\phi} \left[\frac{im}{\sin\theta} P_l^m(\cos\theta) \hat{\theta} + \sin\theta P_l^{m'}(\cos\theta) \hat{\phi} \right], \quad (\text{A2})$$

where $P_l^{m'}(x) \equiv dP_l^m/dx$. Considering the physically relevant case of real $\vec{\xi}$, the fluid motion of a torodial mode on the equatorial plane ($\theta = \pi/2$) is

$$\vec{\xi}_{lm} \sim m \sin m\phi P_l^m(0) \hat{\theta} - \cos m\phi P_l^{m'}(0) \hat{\phi}. \quad (\text{A3})$$

Using the standard transformation between the spherical basis vectors $(\hat{r}, \hat{\theta}, \hat{\phi})$ and the Cartesian one $(\hat{x}, \hat{y}, \hat{z})$, we obtain the following angular dependence of the Cartesian components of $\vec{\xi}_{lm}$ on the equatorial plane:

$$\xi_{lm}^x \sim \cos m\phi \sin\phi P_l^{m'}(0), \quad (\text{A4})$$

$$\xi_{lm}^y \sim -\cos m\phi \cos\phi P_l^{m'}(0), \quad (\text{A5})$$

$$\xi_{lm}^z \sim -m \sin m\phi P_l^m(0). \quad (\text{A6})$$

We see that under a π -rotation ($\phi \rightarrow \phi + \pi$), the Cartesian components transform according to

$$\xi_{lm}^x \rightarrow (-1)^{m+1} \xi_{lm}^x, \quad (\text{A7})$$

$$\xi_{lm}^y \rightarrow (-1)^{m+1} \xi_{lm}^y, \quad (\text{A8})$$

$$\xi_{lm}^z \rightarrow (-1)^m \xi_{lm}^z. \quad (\text{A9})$$